



ELSEVIER

Contents lists available at ScienceDirect

Ultrasonics - Sonochemistry

journal homepage: www.elsevier.com/locate/ultson

Sono-photocatalytic production of hydrogen by interface modified metal oxide insulators

Rushdi D. Senevirathne^a, Lahiru K. Abeykoon^a, Nuwan L. De Silva^a, Chang-Feng Yan^b, Jayasundera Bandara^{a,*}^a National Institute of Fundamental Studies, Hantana Road, CP 20000 Kandy, Sri Lanka^b Hydrogen Production and Utilization Laboratory, Key Laboratory of Renewable Energy, Guangzhou Institute of Energy Conversion Chinese Academic of Sciences, No. 2 Nengyuan Road, Wushan, Tianhe District, Guangzhou 510640, China

ARTICLE INFO

Keywords:

Sono-photocatalysis
MgO
IR photon
Dielectric oxides
Sub-band gap excitations
Multi step excitations

ABSTRACT

Dielectric oxide materials are well-known insulators that have many applications in catalysis as well as in device manufacturing industries. However, these dielectric materials cannot be employed directly in photochemical reactions that are initiated by the absorption of UV–Vis photons. Despite their insensitivity to solar energy, dielectric materials can be made sono-photoactive even for low energy IR photons by modifications of the interfacial properties of dielectric materials by noble metals and metal oxides. In this investigation, by way of interface modification of dielectric MgO nanoparticles by Ag metal and Ag₂O nanoparticles, IR photon initiated sono-photocatalytic activity of MgO is reported. The observed photocatalytic activity is found to be the synergic action of both IR light and sonication effect and sonication assisted a multi-step, sub-bandgap excitation of electrons in the MgO is proposed for the observed catalytic activity of Ag/Ag₂O coated MgO nanoparticles. Our investigation reveals that other dielectric materials such as silver coated SiO₂ and Al₂O₃ also exhibit IR active sono-photocatalytic activity.

1. Introduction

Photocatalytic systems consist of semiconductor particles (photocatalysts) which are in close contact with a liquid or gaseous reaction medium in which the catalytic activity is initiated by using energy from light. When the semiconductor photocatalyst is exposed to light with an appropriate energy, an electron-hole pair is generated by excitation of an electron from the valence band (VB) to the conduction band (CB) [1]. After initial charge separation, the electron in the CB band and the hole in the VB participate in the reduction and oxidation reactions respectively at the semiconductor interface. Important applications of photocatalysis are diverse from environmental remediation [2] (in the treatment of water and air) to alternative fuel [3–5] (photocatalytic hydrogen generation) and hence, photocatalysis reactions have been widely investigated. In photocatalytic reactions, high bandgap semiconductors such as TiO₂, ZnO, SrTiO₃, etc are the commonly used light-harvesting materials due to their appropriate band energy positions for oxidation as well as reduction reactions [6,7].

Among the dielectric oxide materials, SiO₂, ZrO₂, Al₂O₃, and MgO are the most representative materials that have been employed in important technological applications due to their wide band gaps

(6.0–8.0 eV) and thermal stabilities (melting points ~ 2000–2800 °C). However, due to the large bandgap energy, that requires high energy photons (< 5 eV) for electron excitation from the VB to the CB, reactive charge carriers are not generated under direct bandgap excitation with the UV–Vis light [8]. Consequently, no interest has been paid on the use of high bandgap oxides as photocatalysts and only a handful of research articles have been published. In a short recent report, H₂ formation has been noted on SiO₂ and Al₂O₃ nanoparticles under UV irradiation in CH₃OH:H₂O solution and the observed photocatalytic activity has not been attributed to either conventional photocatalysis or a photochemical process [9,10]. Similarly, photocatalytic activities have been reported on MgB₂ under IR and visible light irradiations [10].

Nevertheless, these dielectric materials are one of the most significant and important metal oxides for theoretical and experimental studies due to their unusual stability to photocorrosion. Their optical properties of crystals can be essentially modified by the presence of impurity ions and radiation-induced defects [11]. Due to the presence of extrinsic and intrinsic defects, including those related to surface states in wide bandgap oxides, red-shifted absorptions relative to the fundamental absorption threshold of wide band gap oxides have been noted [12]. This leads to a way of developing wide bandgap solids as

* Corresponding author.

E-mail addresses: jayasundera@yahoo.com, bandaraj@ifs.ac.lk (J. Bandara).

potential competitors for the semiconductor photocatalysts by energy upconversion despite these metal oxides are not active photocatalysts. It is known that ultrasound waves initiate chemical reactions through the acoustic cavitations and the simultaneous use of light and ultrasound irradiation can accelerate the reaction by the synergistic effect of acoustic and solar energy. Hence, sono-photocatalysis is a promising method for the production of hydrogen and degradation of organic and inorganic pollutants present in water [13–16]. Hence, in this investigation, MgO as a model dielectric material, the sono-photocatalytic activity of these high dielectric materials with low-energy IR radiation was demonstrated by modification of interface properties of metal oxide insulators. MgO was selected as a model dielectric compound owing to its simple lattice structure which can be a host for a number of transition metal ions. Properties of MgO nanoparticles were modified by control deposition of Ag and Ag₂O on MgO particles and their sono-photocatalytic activity for hydrogen production with water:methanol mixture by IR radiation was reported.

2. Experimental

Silver oxide coated MgO nanoparticles were prepared by the wet chemical method reported previously [17] and the silver coated MgO catalyst is denoted as Ag(AgO)/MgO hereafter. For the preparation of Ag(AgO)/MgO catalyst, 500 mg of MgO (Sigma-Aldrich, 99% AR) was suspended in 15 ml of dist. H₂O by sonication. For the well dispersed MgO solution, 15 ml of 0.04 M AgNO₃ (BDH, 99%, AR) in water was added with vigorous stirring and stirring was continued for 30 min for better mixing of AgNO₃ with MgO suspension. Then a stoichiometric amount of ammonia solution (BDH, 33%, AR) was added dropwise to the solution for the full conversion of AgNO₃ to Ag₂O. The resulting mixture was heated at 150 °C until the resulting powder gets completely dry. The solution mixture was stirred thoroughly throughout the synthesis to avoid the formation of larger particles. Since the decomposition of Ag₂O to Ag occurs at a temperature over 200 °C, the resultant powder was sintered at 200 °C for 30 min. The prepared Ag (AgO)/MgO catalyst was characterized by X-ray diffraction analysis (XRD), X-ray photoelectron Spectroscopic analysis (XPS), Scanning electron microscopic analysis (SEM), High-resolution transmission electron microscopy (HRTEM), Diffuse reflectance spectroscopy (DRIFT). Chemical composition, the crystal structure of the catalyst were studied by using powder X-ray diffractometer with the PANalytical X'Pert diffractometer (X'Pert PRO MPD, PW3040/60) with Cu-K α ($\lambda = 0.154060$ nm) radiation (40 kV, 40 mA). X-ray diffractograms were obtained before and after the activation of the catalyst. The composition and oxidation states of Ag(AgO)/MgO photocatalyst composite were analyzed by X-ray photoelectron spectroscopy thermo ESCALAB 250XI multifunctional imaging electron spectrometer (Thermo Fisher Scientific Inc.) equipped with an Al K radiation source. The surface morphology of the Ag(AgO)/MgO catalyst was examined by HITACHI SU6600 Variable pressure FE-SEM. Energy dispersive X-ray analysis of Ag₂O/MgO sample was recorded by energy dispersive x-ray diffraction analysis associated with the HITACHI SU6600 FE-SEM scanning electron microscope to find the elemental distribution of the catalyst. The size and morphology of silver nanoparticles were characterized by Transmission electron microscopy (TEM) on a JEM-2100 microscope. The diffuse reflectance spectrum of finely grounded Ag₂O/MgO, photocatalyst was recorded using Shimadzu UV-2450 UV-VIS spectrophotometer in reflectance mode. Diffuse reflectance spectra of MgO and Al₂O₃ was recorded along with Ag₂O for comparison purposes. BaSO₄ was used for the filling of the sample at the reflectance apparatus. Luminescence properties of solid Ag(AgO)/MgO catalyst powder was done using a Shimadzu RF 5000 recording spectrofluorophotometer instruments.

For photocatalytic reaction, finely ground 12.5 mg of Ag(AgO)/MgO catalyst was dispersed in 20 ml of 10% methanol in 25 ml borosilicate flask and tightly sealed with a gas septum. Prior to irradiation, the flask

with catalyst was sonicated for 5 min in a dark room. Then the flask was irradiated with six IR emitting diodes (890 nm) and the experiments were conducted in a dark room to avoid UV and visible light. The sono-photochemical experimental set-up is shown in Fig. S1. The ultrasonic irradiation of the aqueous samples was performed in a 1000 ml stainless steel sonicator bath (15 cm L \times 10 cm W \times 20 cm H) (VWR) at a frequency of 34 kHz with the applied power of 200 ± 3 W at a constant temperature of 30 ± 1 °C. The system was sonicated continuously during irradiation. The gaseous products were quantitatively analyzed using a Shimadzu gas Chromatograph GC-9AM with TCD detector with a packed charcoal column using Ar as the carrier gas. Control experiments were carried out with the IR source in the absence of the catalyst and without IR source in the presence of catalysts. The spectrum and circuit diagram of the IR lamp source used for the irradiation are shown in Fig. S2.

3. Results and discussion

3.1. Characterization of catalyst

The Ag/Ag₂O coated MgO photocatalyst was prepared by controlled deposition of adsorbed Ag⁺ cation on MgO particles surface by the addition of ammonia solution [17]. The catalyst consists of 24% (w/w) of silver (Ag₂O or Ag) and 76% (w/w) of MgO. The formation reactions of Ag/Ag₂O on MgO particle interface is given in the Supporting Information (SI) in detail and the X-ray diffraction patterns of Ag (Ag₂O)/MgO catalyst is shown in Fig. 1. The major diffraction peak at 38.3° can be attributed to both hexagonal Ag₂O (2 0 0) and Ag (1 1 1). [18] The peaks at 53.1°, 65.2° and 70.3° can be attributed to the (2 2 0), (3 1 1) and (2 2 2) plans of cubic Ag₂O respectively (JCPDS No. 72-2108). The peaks located at 64.2° and 77.29° could be attributed to the (2 2 0) and (3 1 1) planes of metallic Ag (JCPDS No. 07-0783) [19]. The characteristic diffraction patterns corresponding to MgO crystalline were observed at $2\theta = 41.25^\circ$ (2 0 0), 62.1° (2 2 0) and 72.6° (3 1 1) [20,21]. Additionally, the presence of diffraction peaks corresponding to amorphous Mg(OH)₂ indicates that some MgO particles contain less crystalline amorphous Mg(OH)₂ particles. Furthermore, as shown in Fig. 1, the similar diffractograms of the Ag(Ag₂O)/MgO catalyst before (Fig. 1a) and after (Fig. 1b) IR irradiation inferred that there is no significant changes occur in the composite structure upon IR irradiation. Also, extra diffraction peaks corresponding to any alloy formation between Ag and Mg were not observed confirming that the catalyst contains only Ag, Ag₂O, and MgO(Mg(OH)₂). Hence, the X-ray

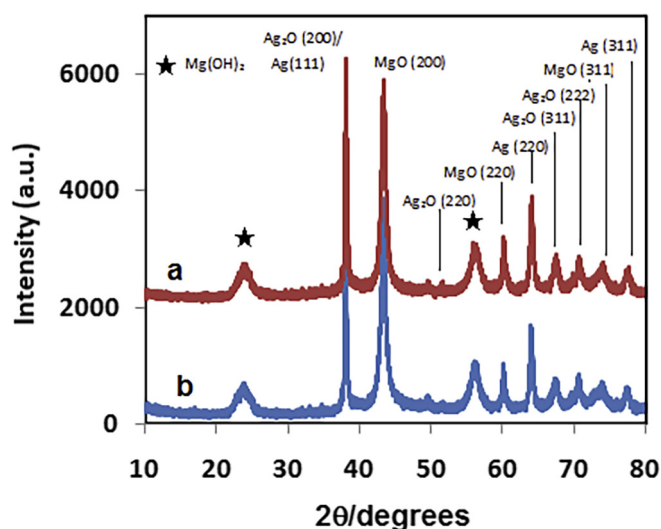


Fig. 1. XRD patterns of Ag(Ag₂O)/MgO (a) before irradiation and (b) after irradiation.

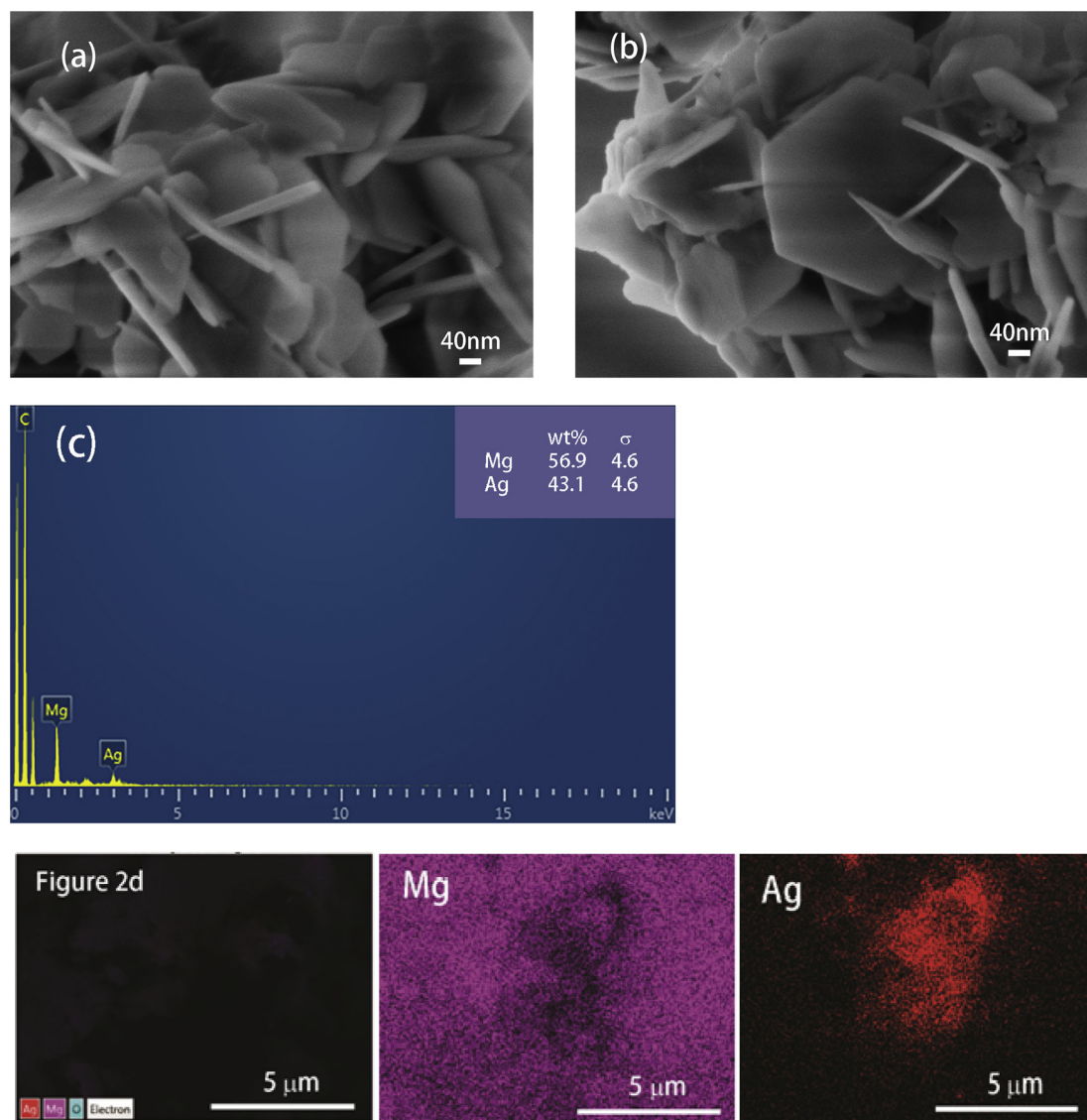
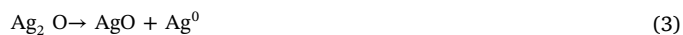


Fig. 2. (a) SEM images of MgO and (b) Ag(Ag₂O)/MgO catalysts: (c) EDS of results Ag(Ag₂O)/MgO catalysts and (d) mapping of Mg and Ag on Ag(Ag₂O)/MgO catalysts:

diffraction analysis of the silver/silver oxide-coated MgO catalyst clearly indicates the presence of both Ag⁰ (silver metal), cubic crystal Ag⁺ (Ag₂O) structures and cubic structure facets of MgO nanoparticles in Ag(Ag₂O)/MgO catalyst.

In the SEM images of MgO and Ag(Ag₂O)/MgO catalysts which are shown in Fig. 2a and b respectively, flake like MgO particles can be observed while no silver nanoparticles were seen on the surface of MgO (Fig. 2b) which could be due to the dispersion of fine silver particles on the high surface area MgO particles. However, EDS results of Ag(Ag₂O)/MgO catalysts (Fig. 2c) indicated that only magnesium, oxygen, and silver elements were present and mapping results of Ag on MgO shown in Fig. 2d clearly demonstrated the uniform distribution of silver particles on MgO nanostructures. The observations of the formation of Ag and Ag₂O nanoparticles on MgO nanoparticles by XRD and SEM analyses are consistent with the TEM results of Ag(Ag₂O)/MgO catalysts, which is shown in Fig. 3. In the HRTEM image of Ag(Ag₂O)/MgO catalyst shown in Fig. 3a, black color particles (intended to be Ag₂O) and light color flake-like particles are MgO while another set of particles are in the quantum dot size which could be due to Ag⁰ particles. The magnified TEM images of the Ag(Ag₂O)/MgO catalyst in 5 nm scale are shown in Fig. 3b and c. The presence of particles with fringe widths of 0.27 nm and 0.24 nm in Fig. 3c confirms the presence of [1 1 1] and

[2 0 0] planes of Ag₂O [22]. On the other hand, the particles with 0.21 nm lattice spacing can be attributed to MgO [2 0 0] lattice plane [23]. Hence, the HTREM, SEM images together with XRD patterns of Ag(Ag₂O)/MgO catalyst clearly demonstrate the presence of Ag and Ag₂O nanostructures on MgO and it can be assumed that during preparation method, Ag and Ag₂O are formed on larger MgO nanocrystallites as given in reactions (1)–(4) (for details, see the SI).



The XPS studies were conducted to confirm the chemical states of Mg and Ag in Ag(Ag₂O)/MgO catalyst. As given in Fig. 4a, in the survey spectrum of Ag(Ag₂O)/MgO catalyst, the characteristic Mg 1s, Ag 3d, C 1s and O 1s peaks could be observed. The high-resolution XPS spectra of Mg 2s peaks and Ag 3d peaks in Ag(Ag₂O)/MgO are shown in Fig. 4b and c respectively. In the high-resolution XPS spectrum shown in Fig. 4b, the peak of the binding energy at 87.5 eV can be assigned to Mg_{2s} (MgO) which is consistent with the analysis results of XRD and

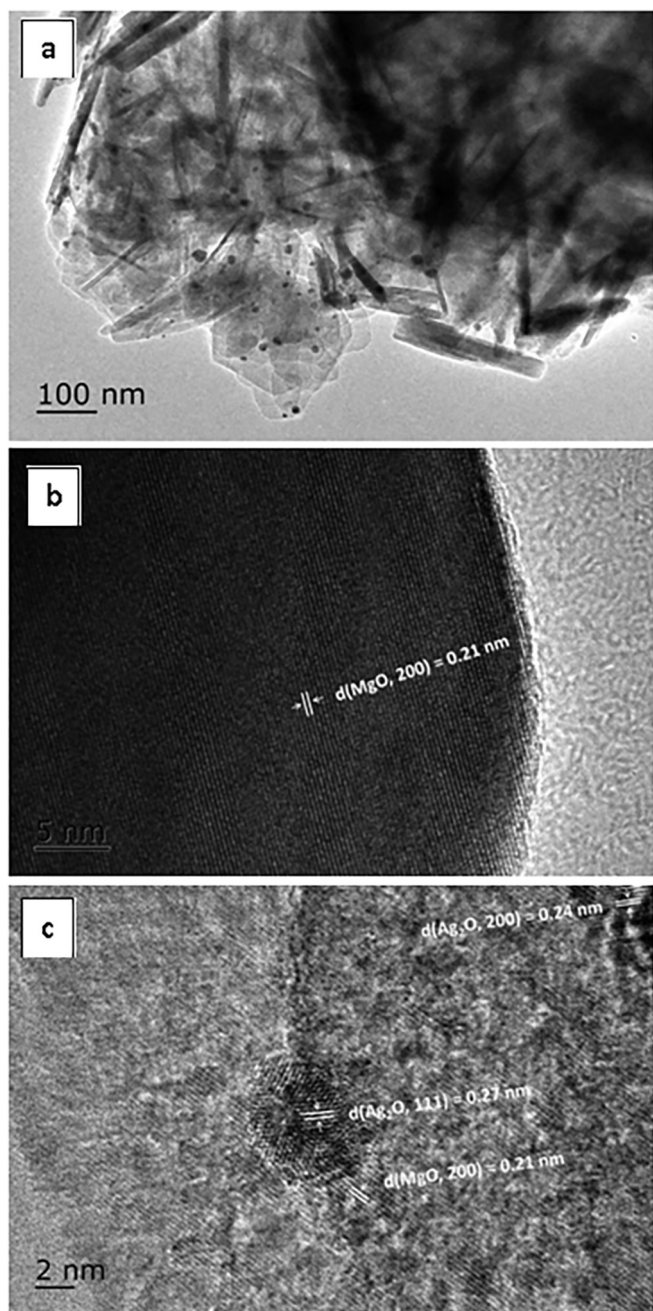


Fig. 3. HRTEM image of (a) Ag(Ag₂O)/MgO catalyst, (b) and (c) the magnified TEM images of the Ag(Ag₂O)/MgO catalyst in 5 nm scale.

TEM [24,25]. Similarly, the observed Ag 3d peaks at 367.6 and 373.5 eV in Fig. 4c, which are due to Ag 3d_{5/2} and 3d_{3/2} respectively confirm the presence of Ag⁺ state as Ag₂O [26]. On the other hand, the peaks at 368.2 and 374.4 which are due to Ag 3d_{5/2} and 3d_{3/2} of metallic silver respectively confirm the presence of Ag⁰ state [26,27]. In each set of peaks the peak separation is about 6 eV which is comparable to the literature reported values. Consequently, with all these observations of TEM, XRD as well as XPS analyses methods it can be confirmed that the catalyst Ag(Ag₂O)/MgO contains homogeneously deposited nanoparticles of Ag⁰ and Ag₂O nanostructures on MgO nanoparticles.

Optical properties of Ag(Ag₂O)/MgO catalyst was studied by diffuse reflectance spectroscopy and shown in Fig. S3. As MgO is a wide-bandgap insulator ($E_g > 7$ eV), optical transitions in the visible range could not be observed in MgO nanostructures [28,29]. However, Ag(Ag₂O)/

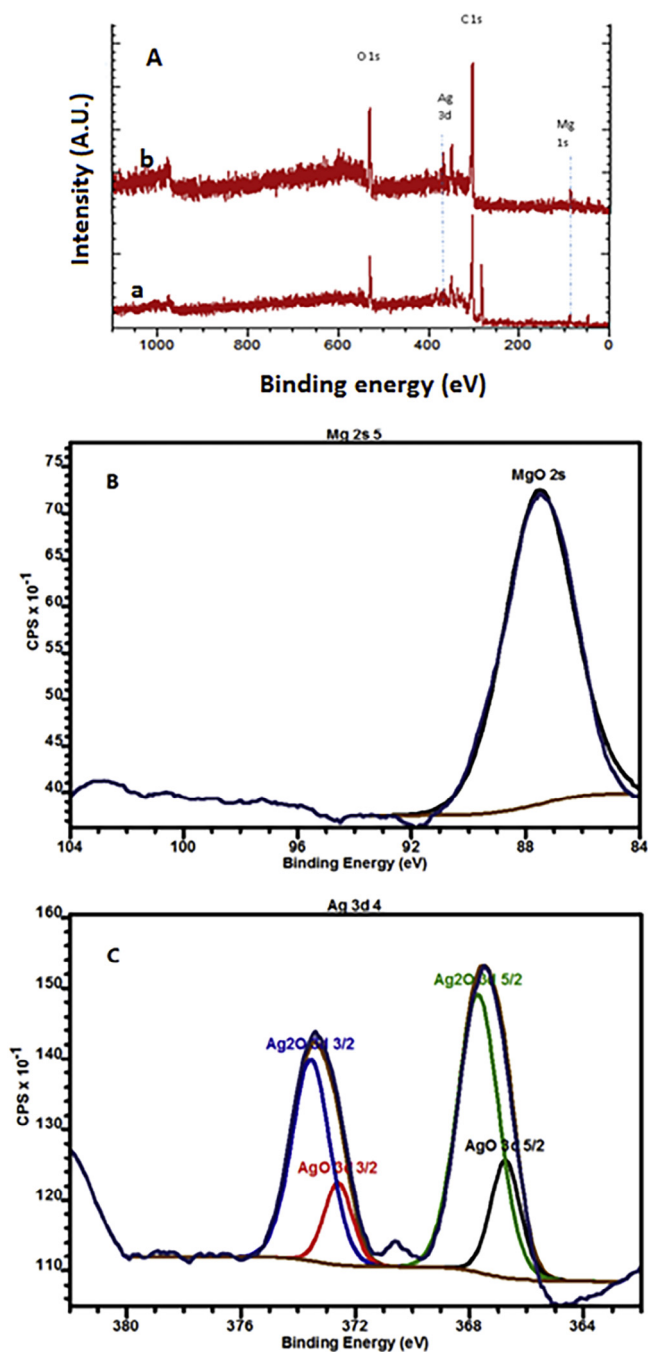


Fig. 4. (A) XPS survey spectrum of Ag(Ag₂O)/MgO, (B) high resolution XPS spectra of Mg 2s and (C) high resolution Ag 3d_{3/2} and 3d_{5/2} peaks in Ag(Ag₂O)/MgO catalyst.

MgO exhibits a broad and weak optical absorption in the visible range from 400 nm to 900 nm. The optical absorption observed for the Ag(Ag₂O)/MgO catalyst may originate either from the sub-bandgap excitation or optical near-field (ONF)-phonon assisted multiphoton excitation process [30–32].

3.2. Sono-photocatalytic activity

When the photocatalyst Ag(Ag₂O)/MgO was irradiated with IR light source in the presence of water:methanol mixture, the formation of hydrogen was noticed with sonication and no hydrogen formation was observed without IR light source or when the irradiation was carried out with the water:methanol solution alone without any catalyst. Also,

Table 1
Hydrogen yield of Ag(Ag₂O)/MgO, Ag(Ag₂O) and MgO with water:methanol mixture under IR irradiation and sonication.

Hydrogen yield (mmol g ⁻¹)				
Ag(Ag ₂ O)/MgO (0.60 g/l)	MgO (0.60 g/l)	Ag ₂ O (0.60 g/l)	Solvent only	Ag(Ag ₂ O)/MgO without IR (0.60 g/l)
0.83 ^a	0.08	0.12	0.002	0.008
2.29 ^b	0.79	0.8	–	–

^a H₂ Yield under atmospheric air.

^b Under Nitrogen saturated conditions.

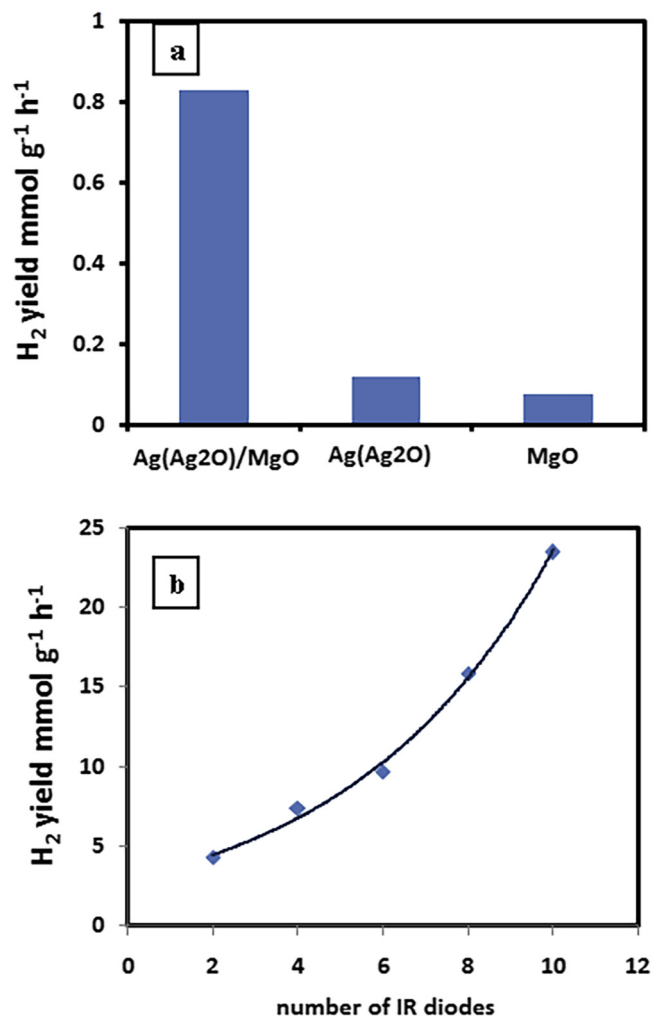


Fig. 5. (a) Hydrogen yield under IR irradiation with Ag(Ag₂O)/MgO, Ag(Ag₂O) and MgO catalyst with water:methanol mixture under sonication. (b) Hydrogen yield of Ag(Ag₂O)/MgO in water:methanol mixture with the variation of IR light intensity under sonication.

no hydrogen was observed with the Ag(Ag₂O)/MgO catalyst under IR irradiation without sonication. These results confirm that the hydrogen is generated with the combined effect of sonolysis as well as photochemical reactions on the catalyst. Under the same reaction conditions in the presence of IR and sonication, MgO or Ag₂O alone produced very low hydrogen amounts compared to Ag(Ag₂O)/MgO catalyst as given in Table 1 and Fig. 5a. i.e. for Ag(Ag₂O)/MgO, MgO and Ag₂O catalysts, hydrogen yields of 0.83, 0.08 and 0.12 mmol g⁻¹ h⁻¹ were noted respectively when these catalysts were irradiated under sonication with IR light source in water: methanol mixture. As given in Table 1,

comparatively higher hydrogen yields were observed for Ag(Ag₂O)/MgO, MgO and Ag₂O catalysts under nitrogen purged system than under air purged conditions which relate to the multi-step excitation process and the detail explanation for the enhanced hydrogen yield under nitrogen will be discussed under reaction mechanism.

In this investigation, photoirradiation was carried out using 6 IR Diodes (6 × 1.6, mW cm⁻²) and the spectrum of the IR source measured from ocean optics QE65 Pro spectrometer is shown in Fig. S2b. The spectral response confirms that the IR light source mainly emits radiation at 880 nm (820–950 nm regions). For further confirmation of the IR photon initiated sono-photocatalytic activity, we studied the IR light intensity dependence on the H₂ production rates of the of Ag(Ag₂O)/MgO catalyst by varying the number of IR diodes at a constant sonication power. As shown in Fig. 5b, the exponential increase in hydrogen production rate with the increase in IR light intensity is a further evidence for the IR photons activated hydrogen production reaction on Ag(Ag₂O)/MgO catalyst. One can argue that the hydrogen could arise due to sonication effect only due to the piezoelectric effect [33]. However, hydrogen would not be produced with MgO or AgO by piezo-catalysis as piezoelectric properties have not been observed either with MgO or Ag₂O [34]. Furthermore, the observation that no hydrogen formation with the catalyst in the absence of IR light and dependence of the hydrogen yield only on light intensity and not on the sonication strength exclude the possibility of formation of hydrogen via a sonication reaction only. A very strong and firm proof for the IR photon initiated photocatalytic activity was demonstrated by the measurement of the Incident Photon to Current Efficiency (IPCE) of Ag(Ag₂O)/MgO catalyst. The IPCE measurements of MgO, Ag/Ag₂O and Ag(Ag₂O)/MgO systems are shown in Fig. 6. In IPCE spectra, it can be clearly observed a weak response of Ag/Ag₂O while MgO alone shows an even weaker response. However, a broad response from 300 to 1100 nm with clear and enhanced responses in the IR and far IR regions observed for Ag(Ag₂O)/MgO confirms the IR response and hence IR initiated photocatalytic activity of Ag(Ag₂O)/MgO.

To rationalize that the observed catalytic activity is not unique to MgO nanoparticles, catalytic activities of similar dielectric metal oxides such as SiO₂ (band gap ~ 7.0 eV) and Al₂O₃ (band gap ~ 8.0 eV) were investigated under sonication with IR radiation. The observed hydrogen yields 0.65 and 0.94 mmol g⁻¹ h⁻¹ respectively for Ag(Ag₂O)/SiO₂ and Ag(Ag₂O)/Al₂O₃ catalysts are comparable to that of Ag(Ag₂O)/MgO catalyst and these results imply that the observed IR photon initiated sono-photocatalytic activity originates exclusively not only on silver oxide-coated MgO catalyst but also on similar silver coated high

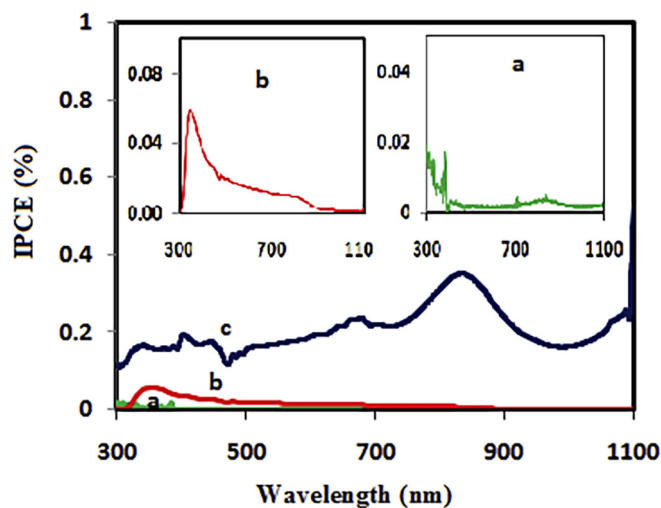


Fig. 6. The IPCE measurements of (a) MgO, (b) Ag/Ag₂O and (c) Ag(Ag₂O)/MgO electrodes. Inset shows the magnified image of IPCE of (a) MgO and (b) Ag/Ag₂O.

bandgap dielectric metal oxide catalysts.

3.3. Reaction mechanism

The sono-photocatalytic activity described above for Ag(Ag₂O)/MgO catalyst substantiate the IR radiation (850 nm, 1.45 eV) initiated sono-photocatalytic activity of Ag(Ag₂O)/MgO catalyst. As described earlier, direct band to band excitations would not be expected both in MgO and Ag₂O nanoparticles with IR photons owing to MgO being a wide-band-gap insulator with $E_g > 7$ eV and Ag₂O being a semiconductor with $E_g > 1.5$ eV [35]. Despite that direct excitation is not energetically possible in both MgO and Ag₂O particles, hydrogen formation was noted when these oxides are subjected to IR radiations under sonication. The enhanced hydrogen yield for Ag(Ag₂O)/MgO catalyst than the individual MgO and Ag₂O powder under the similar reaction condition implies a synergic effect of both MgO and Ag₂O together. Since IR photons do not supply sufficient energy to the electron in the VB for a direct band to band excitation, the other possibility or it can be assumed that the electrons are excited to higher energy states via sub-bandgap excitations. In the process of sub-bandgap excitation, it can be expected that electrons in the VB are excited to an energy position below the energy level of CB by the absorption of IR photon and consequently absorption of another IR photon(s) complete the excitation. We investigated the luminescence spectrum of Ag(Ag₂O)/MgO catalyst to confirm the multistep excitation and as shown in Fig. 7, when the Ag(Ag₂O)/MgO catalyst is excited with 700 nm wavelength, a weak emission signal is observed at ~425 nm. Though the observed emission peak at ~425 nm with the excitation of 700 nm is weak, it is a solid proof for the multistep excitation process.

For sub-bandgap excitation to happen, the materials should possess sufficient sub-energy levels in between VB and CB [30,36]. In fact, most of the oxide materials such as TiO₂ and MgO contain sub-energy levels owing to their crystalline defects and surface states [37]. However sub-bandgap excitations are electric-dipole forbidden [38] and in the following section, the possible scenario for IR photon initiated photocatalytic activity mechanism of Ag(Ag₂O)/MgO catalyst is described. Hence, we propose possible reaction mechanisms as follows;

The possible sub-bandgap excitation mechanism is schematically shown in Fig. 8. In the proposed sub-bandgap excitation method, the electron in the VB should be excited initially to a sub-band level which is dipole-forbidden under normal condition. However, sonication may generate phonons (vibrationally excited state) in MgO and consequently, by the absorption of photons (IR photons in this case), electrons in the phonon states can be excited to higher energy states of Ag

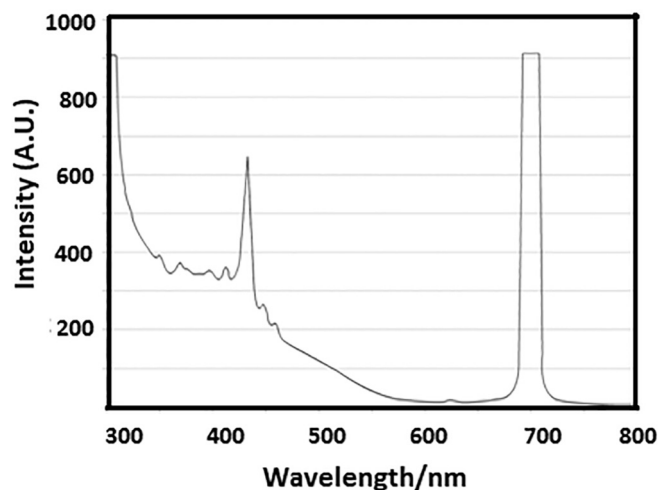


Fig. 7. Luminescence spectra of the catalyst Ag(Ag₂O)/MgO catalyst under excitation at 700 nm.

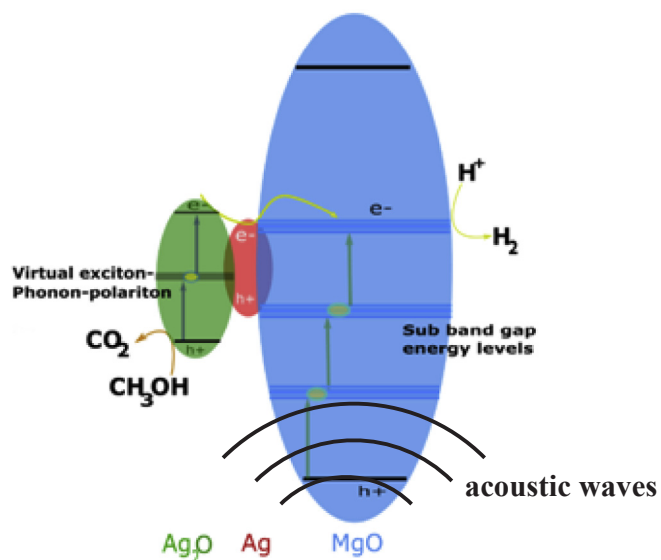


Fig. 8. Schematic presentation of proposed sono-photochemical multistep excitation process in Ag(Ag₂O)/MgO.

(Ag₂O)/MgO catalyst [30,39]. These excited electrons could transfer and trapped in the sub-bandgap levels of MgO and these trapped electrons can be re-excite to higher energy states by the absorption of IR radiation. Once electrons are excited to higher energy states, these photoexcited electrons can participate for the water-splitting reaction producing H₂.

The sono-photocatalytic production of hydrogen demonstrated in this investigation involves multi-step excitation process. In general, water splitting is an uphill task as it involves light-induced single electron transfer with multi-electron catalysis. On the other hand, the Ag(Ag₂O)/MgO catalyst produces hydrogen via multi-step excitation and multi-electron catalysis process. Hence the system must be able to accumulate sufficient excited charges for catalysis reaction and under N₂, charge accumulation can be achieved as it does not consume excited electrons like O₂ molecule does and enhanced higher hydrogen yield under N₂ can be justified. As given in Table 1, the hydrogen yields under nitrogen with MgO and AgO are notably enhanced than that of Ag(Ag₂O)/MgO catalyst. The greater impact of nitrogen on the catalytic process on MgO and AgO than the Ag(Ag₂O)/MgO catalyst implies that the multi-step excitation process is highly retarded or difficult compared to Ag(Ag₂O)/MgO catalyst.

4. Conclusions

The photo-inactive dielectric materials such as MgO, SiO₂, and Al₂O₃ can be made photoactive by the synergic effect of both acoustic energy and photon energy. The noble metal decorated dielectric materials are capable of producing hydrogen by combined IR photons and sonochemical reactions in water; methanol mixture. The sono-photocatalysis with dielectric materials was less significant and hardly observed in the absence of noble metal and metal oxides (i.e. Ag metal and Ag₂O nanoparticles) on the interface of the dielectric nanoparticles. The observed photocatalytic activity of noble metal and metal oxides decorated dielectric materials is found to be the synergic action of both IR light and sonication effect and sonication assisted a multi-step, sub-bandgap excitation of electrons in the MgO is proposed for the observed catalytic activity of Ag/Ag₂O coated MgO nanoparticles.

Acknowledgments

J.B. appreciates the Chinese Academy of Sciences (CAS) for providing him a CAS President's International Fellowship for Visiting

Scientists (PIFI). Technical support from D. Aluthpatabendi is highly appreciated.

Appendix A. Supplementary data

Supplementary data associated with this article can be found, in the online version, at <https://doi.org/10.1016/j.ultsonch.2018.03.016>.

References

- [1] F. Wang, C. Di Valentin, G. Pacchioni, Doping of WO_3 for photocatalytic water splitting: hints from density functional theory, *J. Phys. Chem. C* 116 (2012) 8901–8909.
- [2] V. Madhavi, P. Kondaiah, G. Mohan Rao, Influence of silver nanoparticles on titanium oxide and nitrogen doped titanium oxide thin films for sun light photocatalysis, *Appl. Surf. Sci.* 436 (2018) 708–719.
- [3] G. Iervolino, I. Tantis, L. Sygellou, V. Vaiano, D. Sannino, P. Lianos, Photocurrent increase by metal modification of Fe_2O_3 photoanodes and its effect on photoelectrocatalytic hydrogen production by degradation of organic substances, *Appl. Surf. Sci.* 400 (2017) 176–183.
- [4] L.-C. Pop, V. Dracopoulos, P. Lianos, Photoelectrocatalytic hydrogen production using nanoparticulate titania and a novel Pt/carbon electrocatalyst: the concept of the “Photoelectrocatalytic Leaf”, *Appl. Surf. Sci.* 333 (2015) 147–151.
- [5] R. Sivakumar, J. Thomas, M. Yoon, Polyoxometalate-based molecular/nano composites: advances in environmental remediation by photocatalysis and biomimetic approaches to solar energy conversion, *J. Photochem. Photobiol. C* 13 (2012) 277–298.
- [6] X.W. Wang, G. Liu, L.Z. Wang, Z.G. Chen, G.Q. Lu, H.M. Cheng, ZnO-CdS@Cd heterostructure for effective photocatalytic hydrogen generation, *Adv. Energy Mater.* 2 (2012) 42–46.
- [7] A. Hernández-Ramírez, I. Medina-Ramírez, *Semiconducting materials, Photocatalytic Semiconductors*, Springer, 2015, pp. 1–40.
- [8] C. Anastasescu, M. Zaharescu, D. Angelescu, C. Munteanu, V. Bratan, T. Spataru, C. Negrița, N. Spataru, I. Balint, Defect-related light absorption, photoluminescence and photocatalytic activity of SiO_2 with tubular morphology, *Sol. Energy Mater. Sol. Cells* 159 (2017) 325–335.
- [9] R.G. Li, X.L. Wang, S.Q. Jin, X. Zhou, Z.C. Feng, Z. Li, J.Y. Shi, Q. Zhang, C. Li, Photo-induced H_2 production from a $\text{CH}_3\text{OH-H}_2\text{O}$ solution at insulator surface, *Sci. Rep.* 5 (2015).
- [10] V.G. Kravets, A.N. Grigorenko, New class of photocatalytic materials and a novel principle for efficient water splitting under infrared and visible light: MgB_2 as unexpected example, *Opt. Express* 23 (2015) A1651–A1663.
- [11] X.F. Zong, C.F. Shen, S. Liu, Z.C. Wu, Y. Chen, Radiation-induced electrical degradation in crystalline Al_2O_3 , *Phys. Rev. B* 49 (1994) 15514–15524.
- [12] K.P. McKenna, Electronic and chemical properties of a surface-terminated screw dislocation in MgO , *J. Am. Chem. Soc.* 135 (2013) 18859–18865.
- [13] C.G. Joseph, G. Li Puma, A. Bono, D. Krishnaiah, Sonophotocatalysis in advanced oxidation process: a short review, *Ultrason. Sonochem.* 16 (2009) 583–589.
- [14] K.P. Jyothi, S. Yesodharan, E.P. Yesodharan, Ultrasound (US), Ultraviolet light (UV) and combination (US + UV) assisted semiconductor catalysed degradation of organic pollutants in water: oscillation in the concentration of hydrogen peroxide formed in situ, *Ultrason. Sonochem.* 21 (2014) 1787–1796.
- [15] M. Ahmad, E. Ahmed, Z.L. Hong, W. Ahmed, A. Elhissi, N.R. Khalid, Photocatalytic, sonocatalytic and sonophotocatalytic degradation of Rhodamine B using ZnO/CNTs composites photocatalysts, *Ultrason. Sonochem.* 21 (2014) 761–773.
- [16] M. Penconi, F. Rossi, F. Ortica, F. Elisei, P.L. Gentili, Hydrogen production from water by photolysis, sonolysis and sonophotolysis with solid solutions of rare earth, gallium and indium oxides as heterogeneous catalysts, *Sustainability* 7 (2015) 9310–9325.
- [17] A. Gannoruwa, K. Niroshan, O. Ileruma, J. Bandara, Infrared radiation active, novel nanocomposite photocatalyst for water splitting, *Int. J. Hydrogen Energy* 39 (2014) 15411–15415.
- [18] Z. Zhang, L. Zhang, S. Wang, W. Chen, Y. Lei, A convenient route to polyacrylonitrile/silver nanoparticle composite by simultaneous polymerization–reduction approach, *Polymer* 42 (2001) 8315–8318.
- [19] G.I. Waterhouse, G.A. Bowmaker, J.B. Metson, The thermal decomposition of silver (I, III) oxide: a combined XRD, FT-IR and Raman spectroscopic study, *Phys. Chem. Chem. Phys.* 3 (2001) 3838–3845.
- [20] T. Yoshida, T. Tanaka, H. Yoshida, T. Funabiki, S. Yoshida, T. Murata, Study of dehydration of magnesium hydroxide, *J. Phys. Chem.* 99 (1995) 10890–10896.
- [21] Y. Liu, Q. Li, S. Gao, J.K. Shang, Exceptional As(III) sorption capacity by highly porous magnesium oxide nanoflakes made from hydrothermal synthesis, *J. Am. Ceram. Soc.* 94 (2011) 217–223.
- [22] M.A.M. Khan, S. Kumar, M. Ahamed, S.A. Alrokayan, M.S. AlSalhi, Structural and thermal studies of silver nanoparticles and electrical transport study of their thin films, *Nanoscale Res. Lett.* 6 (2011) 434.
- [23] K. Nagashima, T. Yanagida, H. Tanaka, T. Kawai, Epitaxial growth of MgO nanowires by pulsed laser deposition, *J. Appl. Phys.* 101 (2007) 4.
- [24] N.C. Haider, J. Alonso, W.E. Swartz, Valence and core electron spectra of Mg in MgO in evaporated thin films, *Z. Naturforsch. A* (1975) 1485.
- [25] B.V. Crist, D.B. Crist, *Handbook of Monochromatic XPS Spectra*, Wiley, New York, 2000.
- [26] J.F. Weaver, G.B. Hoflund, Surface characterization study of the thermal-decomposition of Ag_2O , *Chem. Mater.* 6 (1994) 1693–1699.
- [27] H. Zhang, G. Wang, D. Chen, X.J. Lv, U.H. Jinghong, Tuning photoelectrochemical performances of Ag-TiO_2 nanocomposites via reduction/oxidation of Ag, *Chem. Mater.* 20 (2008) 6543–6549.
- [28] K. Mageshwari, S.S. Mali, R. Sathyamoorthy, P.S. Patil, Template-free synthesis of MgO nanoparticles for effective photocatalytic applications, *Powder Technol.* 249 (2013) 456–462.
- [29] J. Narayan, R.A. Weeks, E. Sonder, Aggregation of defects and thermal-electric breakdown in MgO , *J. Appl. Phys.* 49 (1978) 5977–5981.
- [30] T. Yatsui, T. Imoto, T. Mochizuki, K. Kitamura, T. Kawazoe, Dressed-phonon (DPP)-assisted visible-and infrared-light water splitting, *Sci. Rep.* 4 (2014).
- [31] W.-J. Kuang, Q. Li, Y.-X. Chen, K. Hu, N.-H. Wang, F.-L. Xing, Q. Yan, S.-S. Sun, Y. Huang, Y. Tao, Surface exciton emission of MgO crystals, *J. Phys. D: Appl. Phys.* 46 (2013) 365501.
- [32] A. Gannoruwa, B. Ariyasinghe, J. Bandara, The mechanism and material aspects of a novel $\text{Ag}_2\text{O/TiO}_2$ photocatalyst active in infrared radiation for water splitting, *Catal. Sci. Technol.* 6 (2016) 479–487.
- [33] M.B. Starr, J. Shi, X. Wang, Piezopotential-driven redox reactions at the surface of piezoelectric materials, *Angew. Chem. Int. Ed.* 51 (2012) 5962–5966.
- [34] S. Ikeda, T. Takata, M. Komoda, M. Hara, J.N. Kondo, K. Domen, A. Tanaka, H. Hosono, H. Kawazoe, Mechano-catalysis—a novel method for overall water splitting, *PCCP* 1 (1999) 4485–4491.
- [35] T. Kotani, Exact exchange-potential band-structure calculations by the LMTO-ASA method: MgO and CaO , *Phys. Rev. B* 50 (1994) 14816.
- [36] S. Rühl, L. Van Vugt, H.-Y. Li, N. Keizer, L. Kuipers, D. Vanmaekelbergh, Nature of sub-band gap luminescent eigenmodes in a ZnO nanowire, *Nano Lett.* 8 (2008) 119–123.
- [37] J. Zhang, P. Zhou, J. Liu, J. Yu, New understanding of the difference of photocatalytic activity among anatase, rutile and brookite TiO_2 , *PCCP* 16 (2014) 20382–20386.
- [38] Y. Li, W. Yin, R. Deng, R. Chen, J. Chen, Q. Yan, B. Yao, H. Sun, S.-H. Wei, T. Wu, Realizing a SnO_2 -based ultraviolet light-emitting diode via breaking the dipole-forbidden rule, *NPG Asia Mater.* 4 (2012) e30.
- [39] B. Dinda, *Essentials of Pericyclic and Photochemical Reactions*, Springer, 2017.